



## Conjugate Natural Convection Heat Transfer in a Cavity with Arc-Shaped Partition with Different Materials

*Farklı Malzemelerden Oluşan Açılı Şekillendirilmiş Bölmeler ile Bir Hacimdeki Birleşik Doğal Taşınım Isı Transferi*

Mert Gürtürk<sup>1\*</sup>, Hakan Fehmi Öztop<sup>2</sup>, Khaled Al-Salem<sup>3</sup>

<sup>1</sup>Department of Mechanical Education, Technical Education Faculty, Fırat University, Elazığ, Turkey

<sup>2</sup>Department of Mechanical Engineering, Technology Faculty, Fırat University, Elazığ, Turkey

<sup>3</sup>Department of Mechanical Engineering, Engineering College, King Saud University, Riyadh, Saudi Arabia

### Abstract

In this numerical study, the effects of inserting conductive arc-shaped baffles in a differentially heated, square cavity on natural convection heat transfer are investigated. The baffles are made from different materials such as aluminum, steel and wood. Rayleigh number is varied from  $7 \cdot 10^4$  to  $4 \cdot 10^6$ . The nondimensional radius of the baffle is also varied from  $R=0$  (without partition) to  $R=1.12$ . The Fluent commercial code with Finite volume method is used to solve the governing equations of flow and heat transfer. It is observed that heat transfer, temperature distribution and fluid flow are affected by changing the radius of the partition with the maximum heat transfer obtained at  $R=1$ .

**Keywords:** Arc-shaped baffle, Conjugate heat transfer, Natural convection

### Öz

Bu nümerik çalışmada, boş bir kare içerisine yerleştirilen farklı yarıçaplardaki engellerin, doğal taşınım üzerindeki etkileri incelenmiştir. Kullanılan engeller farklı materyallerden tercih edilmiştir. Bu materyaller alüminyum, çelik ve tahtadır. Rayleigh sayısı  $7 \cdot 10^4$ 'den,  $4 \cdot 10^6$ 'ya değişmektedir. Yerleştirilen engellerin boyutsuz yarıçapları,  $R=0$ 'dan (engelsiz),  $R=1.12$ 'ye kadar değiştirilmiştir. Sonlu hacim metodu, Fluent ticari kodu kullanılarak, ısı transferi ve momentum denklemleri çözümlenmiştir. Yerleştirilen engellerin yarıçapındaki değişiklik, kare içerisindeki akış ve sıcaklık dağılımını etkilemiş ve  $R=1$ 'de en fazla ısı transferinin elde edildiği gözlemlenmiştir.

**Anahtar Kelimeler:** Açılı şekillendirilmiş engel, Birleşik ısı transferi, Doğal taşınım

### 1. Introduction

Natural convection heat transfer is encountered in many engineering applications such as cooling of electronic devices, solar collectors, building heating and cooling, and heat exchangers. It can be controlled, passively, in enclosures using a number of elements such as flow deviators, different shaped baffles, or partitions. These passive elements can be adiabatic or conductive. The use of partitions to control natural convection heat transfer is not a new idea. Lin and Bejan (1983) and Nishimura et al. (1989) investigated, numerically, the natural convection heat transfer in a partitioned

enclosure. Costa et al. (2003) studied heat convection in an enclosure with rectangular partitions of finite thickness. The position, length and thermal conductivity of the partitions are varied. Kuznetsov and Sheremet (2010) and Al-Amiri et al. (2009) investigated the effect of thermal conductivity of the partitions on heat transfer inside the enclosure. Tasnim and Collins (2005) investigated, numerically, the natural convection in a square cavity with an adiabatic arc shaped baffle. They observed changes in the flow and thermal fields caused by the obstruction of the baffle. Oztop et al. (2011) studied conjugate heat transfer in air filled tube inserted inside a cavity. The walls of the tube were considered thermally conductive. In this study, the effects of arc shaped conductive baffles on natural convection heat transfer in a square enclosure are studied. The results are presented in the form of streamlines, isotherms, local and average Nusselt

\*Corresponding Author: [m.gurturk@gmail.com](mailto:m.gurturk@gmail.com)

Received / Geliş tarihi : 29.03.2016

Accepted / Kabul tarihi : 28.10.2016

numbers. In this study and similar studies particularly have been focused on the cooling of electronic devices. Also, different application fields such as building heating, cooling and heat exchangers are considered this study and similar studies for control natural convection heat transfer.

## 2. Material and Methods

In this part of the study, considered model, governing equations, numerical procedure, and validation are presented, but before all, the model is explained.

### 2.1. Considered Model

The physical model considered in this study is depicted in Figure 1 (a) and consists of a square cavity with  $H = L$  and the vertical walls are kept at constant temperature. The temperature of the left wall is higher than that of the right wall. The horizontal walls are adiabatic. The gravity acts in the  $-y$  direction. The cavity has two arc-shaped baffles made from different materials with different values of thermal conductivity. The radius of curvature of the baffles is varied. Figure 1 (b) gives grid distribution.

Regular grid is used in this work as shown from the figure. A regular grid is increased the mesh number from 5238 to 20123. The grid number is determined as 10201. Why the authors chose the given grid structure explained in the validation part of this study.

### 2.2. Governing Equations

The governing equations to describe the considered problem are based on the conservation laws of mass, momentum and energy. The Boussinesq approximation is applied. The

radiation mode of heat transfer, viscous dissipation and pressure work are neglected. With these assumptions, the governing equations can be written as,

$$\frac{\partial u}{\partial x} + \frac{\partial v}{\partial y} = 0 \tag{1}$$

$$u \frac{\partial u}{\partial x} + v \frac{\partial u}{\partial y} = -\frac{1}{\rho} \frac{\partial p}{\partial x} + \nu \left( \frac{\partial^2 u}{\partial x^2} + \frac{\partial^2 v}{\partial y^2} \right) \tag{2}$$

$$u \frac{\partial v}{\partial x} + v \frac{\partial v}{\partial y} = -\frac{1}{\rho} \frac{\partial p}{\partial y} + \nu \left( \frac{\partial^2 v}{\partial x^2} + \frac{\partial^2 v}{\partial y^2} \right) + g\beta(T - T_c) \tag{3}$$

$$u \frac{\partial T}{\partial x} + v \frac{\partial T}{\partial y} = \frac{k}{\rho C_p} \left( \frac{\partial^2 T}{\partial x^2} + \frac{\partial^2 T}{\partial y^2} \right) \tag{4}$$

For solid region,

$$\frac{\partial^2 T}{\partial x^2} + \frac{\partial^2 T}{\partial y^2} = 0 \tag{5}$$

The governing equations in terms of velocity and pressure can be written in a dimensionless form as,

$$\frac{\partial U}{\partial X} + \frac{\partial V}{\partial Y} = 0 \tag{6}$$

$$U \frac{\partial U}{\partial X} + V \frac{\partial U}{\partial Y} = -\frac{\partial P}{\partial X} + Pr \left( \frac{\partial^2 U}{\partial X^2} + \frac{\partial^2 U}{\partial Y^2} \right) \tag{7}$$

$$U \frac{\partial V}{\partial X} + V \frac{\partial V}{\partial Y} = -\frac{\partial P}{\partial Y} + Pr \left( \frac{\partial^2 V}{\partial X^2} + \frac{\partial^2 V}{\partial Y^2} \right) + RaPr\theta \tag{8}$$

$$U \frac{\partial \theta}{\partial X} + V \frac{\partial \theta}{\partial Y} = \left( \frac{\partial^2 \theta}{\partial X^2} + \frac{\partial^2 \theta}{\partial Y^2} \right) \tag{9}$$

For solid region,

$$\frac{\partial^2 \theta}{\partial x^2} + \frac{\partial^2 \theta}{\partial y^2} = 0 \tag{10}$$

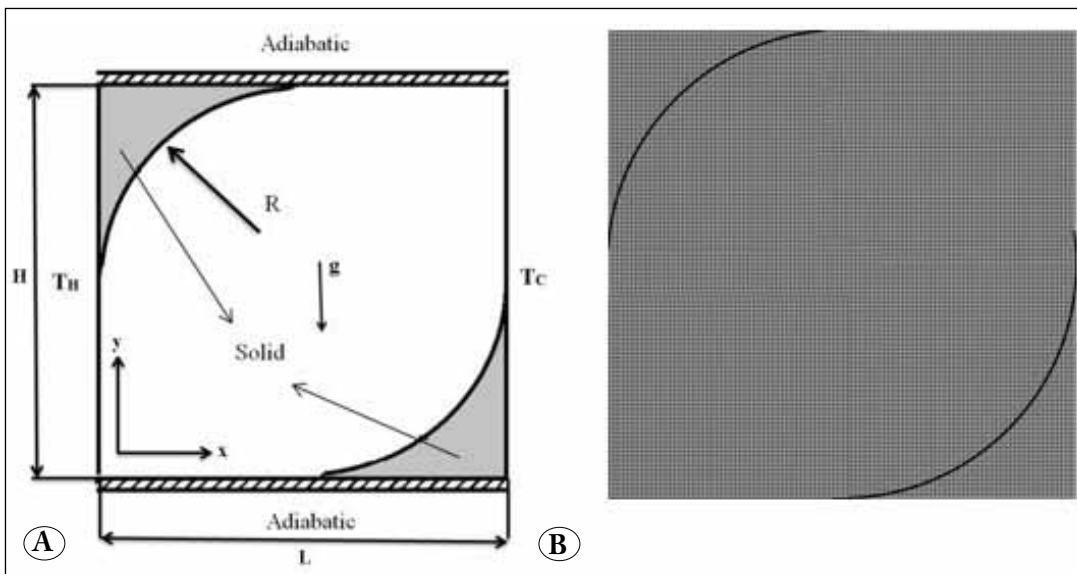


Figure 1. A) Physical model, B) Grid distribution.

Where the flowing dimensionless variables have been used:

$$X = \frac{x}{L}, Y = \frac{y}{L}, U = \frac{uL}{\alpha}, V = \frac{vL}{\alpha}, P = \frac{(p + \rho g y)}{\rho v^2}, \quad (11)$$

$$\theta = \frac{T - T_c}{T_h - T_c}$$

Boundary conditions are written as,

Left wall

$$\chi = 1, 0 \leq Y \leq 1, U = 0, V = 0, \theta = 1 \quad (12)$$

Right wall

$$\chi = 0, 0 \leq Y \leq 1, U = 0, V = 0, \theta = 0 \quad (13)$$

Top and bottom walls

$$0 \leq X \leq 1, Y = 0, U = 0, V = 0, \frac{\partial \theta}{\partial Y} = 0 \quad (14)$$

The arc-shaped partition has conductive thermal boundary condition as,

$$k_{fluid} \left( \frac{\partial \theta}{\partial n} \right)_{fluid} = k_{solid} \left( \frac{\partial \theta}{\partial n} \right)_{solid} \quad (15)$$

$$T_{fluid} = T_{solid} \quad (16)$$

Definition of Prandtl number, Grashof number and Rayleigh number are given as

$$Pr = \frac{\nu}{\alpha}, Gr = \frac{g\beta\Delta TH^3}{\nu^2}, Ra = Gr.Pr \quad (17)$$

### 2.3. Numerical Procedure

The finite volume method is used to solve the governing equations. The SIMPLE algorithm is used to treat the pressure term (Patankar 1980). QUICK scheme (Hayasse et al. 1992) is used for the discretization of the convective terms in the momentum and energy equations. The calculations are done using FLUENT (Fluent 2009) commercial software.

The local Nusselt number is calculated from the hot vertical surface as,

$$Nu_w = - \frac{\partial \theta}{\partial X} \Big|_{X=0} \quad (18)$$

and the average Nu as,

$$Nu_{ave} = \int_0^H Nu_w dy \quad (19)$$

**Table 1.** Comparison of average nusselt number with literature.

Average Nu number	Ra=10 <sup>4</sup>	Ra=10 <sup>5</sup>	Ra=10 <sup>6</sup>
Wan et al. (2001)	2.254	4.598	8.976
Barakos et al. (1994)	2.245	4.510	8.806
Present Study	2.235	4.509	8.904

### 2.4. Validation

As a solution scheme a commercial code is used but the grid is validated by solving the differentially heated enclosure problem without the baffles and comparing the calculated Nu number with the published data (Wan et al. 2001 and Barakos et al. 1994). Table 1 shows good agreement with the published data.

### 3. Results and Discussion

A computational study has been performed to investigate the effects of arc-shaped baffles, which are made of different materials, on natural convection heat transfer and fluid flow. The main control parameters are the radius of curvature of the arc-shaped baffles, material of the baffles and Rayleigh number. Prandtl number is taken as 0.7 for all cases.

Figure 2 (a - c) show the streamlines (on the left) and isotherms (on the right) for Ra=7.10<sup>4</sup> and R=1 with baffles of different materials. With the baffles in place, as shown in Figure 2 (b), the streamlines are rotated with a slight angle towards the baffle-free corners. The shape of outer streamlines matches the geometry of the inner perimeter of the enclosure due to the streamlined edges of the baffles. This is thought to reduce flow friction. Due to the heat differential between the vertical walls, the heated air moves from the bottom left corner to the top right. Isotherms are distributed as parallel to the vertical walls inside the partition due to conduction. Higher temperature values are observed inside the baffles. The streamlines show that baffle material has little effect on the fluid flow. Temperature values inside the baffle are decreased with increasing of thermal conductivity of the baffle. For aluminum baffles, temperature is almost constant inside the baffle due to high conductivity.

Figure 3 (a - c) show the streamlines (on the left) and isotherms (on the right) for Ra=6.10<sup>5</sup> and R=1 for different materials of the baffles. In this case, two cells are formed inside the cavity and both turn in the same direction. Due to streamlined structure of the baffles, the center cells take a circular shape. The isotherms are also pressed against the

isothermal walls before moving horizontally inside the enclosure.

As Ra number is increased, both thermal and velocity boundary layers becomes thinner as seen in Figure 4. The isotherms show that convection becomes stronger at the middle of the cavity. Based on mid-axis in x-direction there is a symmetrical distribution for both flow and temperature distribution. The type of baffle material becomes more important for higher values of Rayleigh number.

Figures 5 – 7 illustrate the variation of local Nusselt number with different parameters such as Rayleigh number, material and radius of curvature of baffle. Local Nusselt number values are calculated along the hot surface as in Eq. (18). As can be seen from the figures, using baffles made of higher thermal conductivity material, such as aluminum and steel, lead to higher heat transfer ratio near the bottom side of

the enclosure. This indicates that the presence of the baffles enhances the local heat transfer. The material of the baffles and the radius of curvature controls the enhancements of heat transfer in the enclosure. Higher heat transfer is observed with increasing of Rayleigh number.

Variation of average Nusselt number with different radius and materials of baffles at different values of Rayleigh number is presented in Fig. 8. As seen from the figure, thermal conductive coefficient of the material is an effective control parameter for heat transfer for all values of Rayleigh number with wooden baffles causing the least heat transfer. For all values of Rayleigh number, heat transfer reaches a maximum at  $R=1$  due to space limitation inside the cavity. This result is supported by Refs. (Chamkha and Ismail 2013, Chamkha and Ismail 2013).

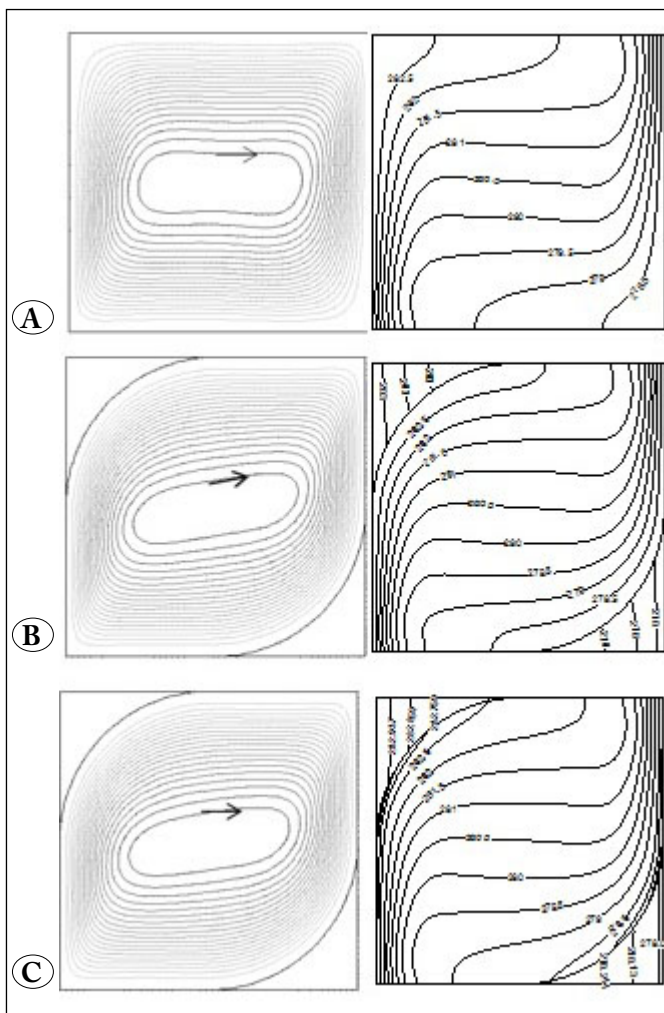


**Figure 2.** Streamlines (on the left) and isotherms (on the right)  $Ra=7 \cdot 10^4$  and  $R = 1$ , **A)** Without baffles, **B)** Aluminum, **C)** Wood.

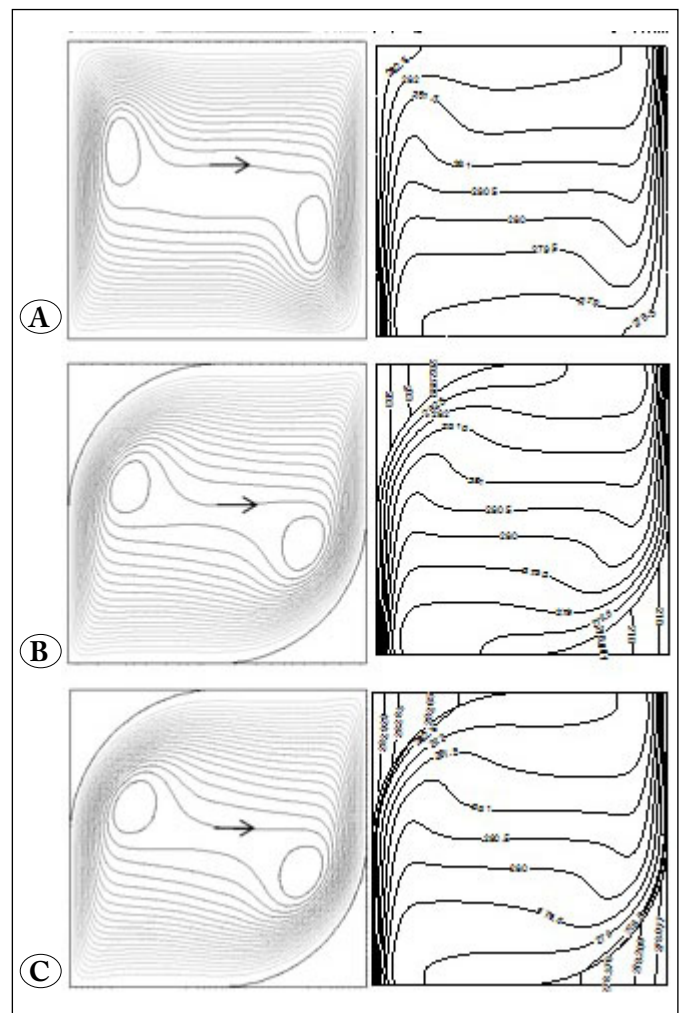


**Figure 3.** Streamlines (on the left) and isotherms (on the right)  $Ra=6 \cdot 10^5$  and  $R=1$ , **A)** Without partition, **B)** Aluminum, **C)** Wood

### 4. Conclusions

The important findings from this study can be summarized in the following:

- Arc-shaped baffles can be used as heat and flow control elements.
- For all values of Rayleigh numbers, the highest heat transfer was obtained at  $R=1$ .
- The thermal conductivity of the baffle material has an effect on heat transfer inside the enclosure. The higher the thermal conductivity the higher the heat transfer.

### Nomenclature

$A$  aspect ratio,  $H/L$

$g$  acceleration due to gravity,  $m/s^2$

$H$  height of enclosure,  $m$

$k$  Thermal conductivity,  $W/m \times K$

$L$  length of enclosure,  $m$

$Nu$  Nusselt number

$p$  pressure,  $N/m^2$

$P$  dimensionless pressure

$Pr$  Prandtl number

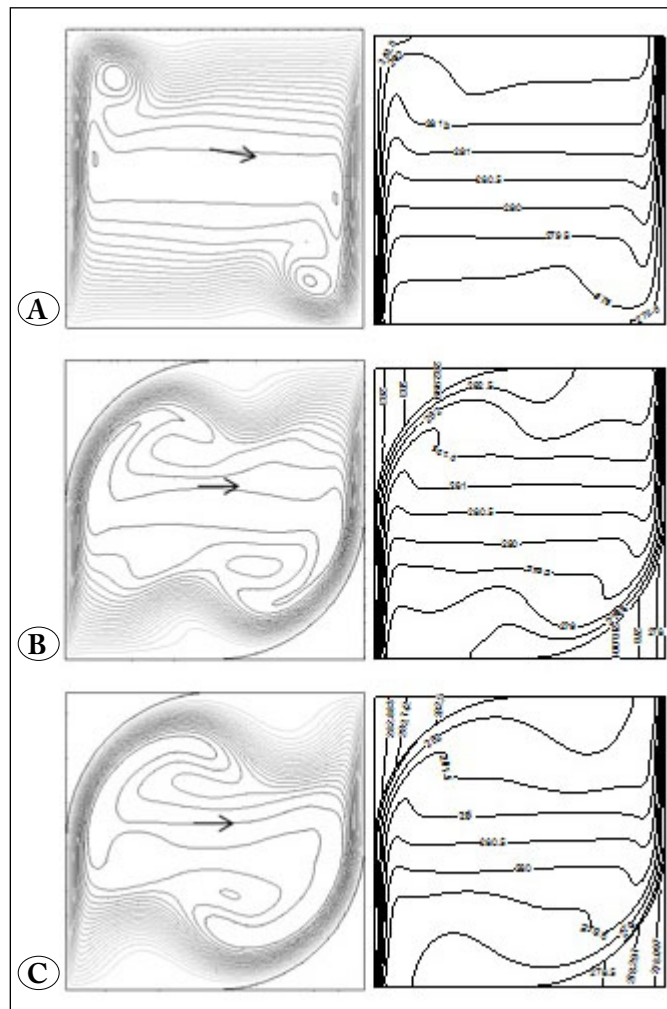


**Figure 4.** Streamlines (on the left) and isotherms (on the right)  $Ra=4 \cdot 10^6$  and  $R=1$ , **A)** Without partition, **B)** Aluminum, **C)** Wood.

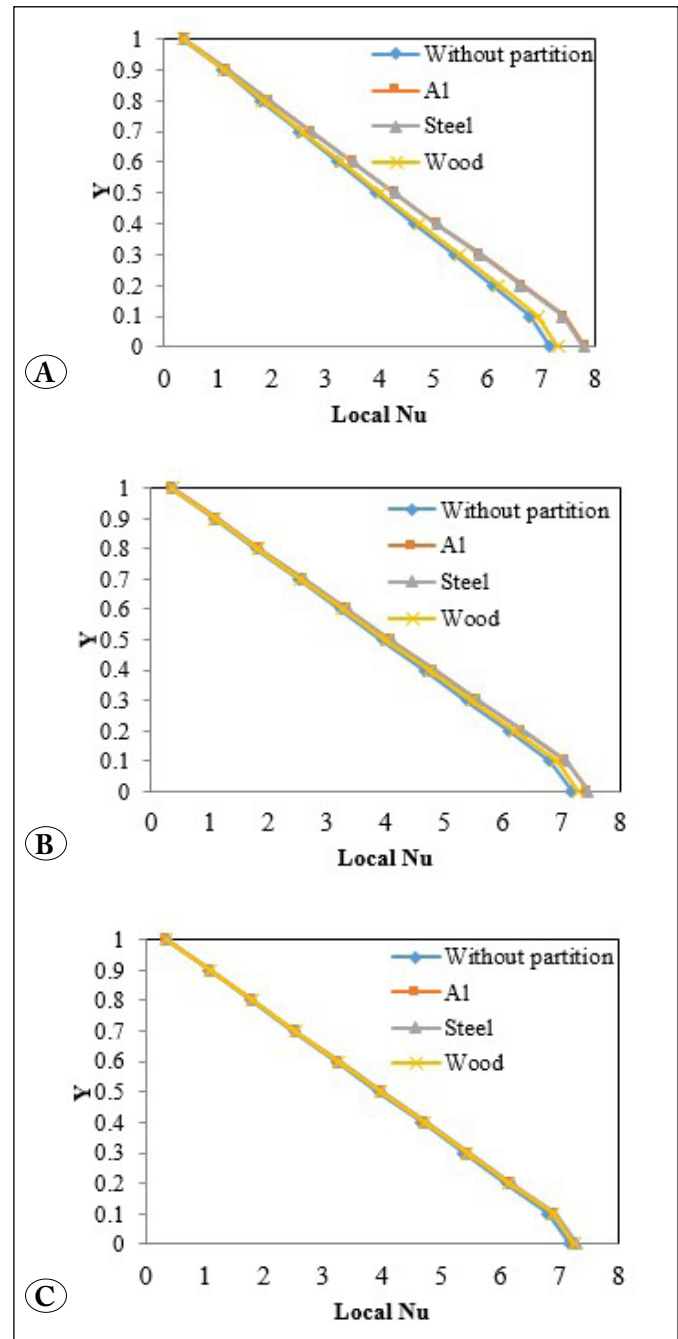


**Figure 5.** Variation of local Nusselt number along the vertical direction for  $Ra = 7 \cdot 10^4$ , **A)**  $R=1$ , **B)**  $R=1.1$ , **C)**  $R=1.12$ .

$T$  dimensionless temperature  
 $T_c$  temperature of the cold wall, °C  
 $T_b$  temperature of the hot wall, °C  
 $U$  dimensionless axial velocity  
 $u$  dimensional axial velocity  
 $V$  dimensionless vertical velocity

$v$  dimensional vertical velocity  
 $x$  dimensional axial coordinate  
 $X$  dimensionless axial coordinate,  
 $y$  dimensional vertical coordinate  
 $Y$  dimensionless vertical coordinate,

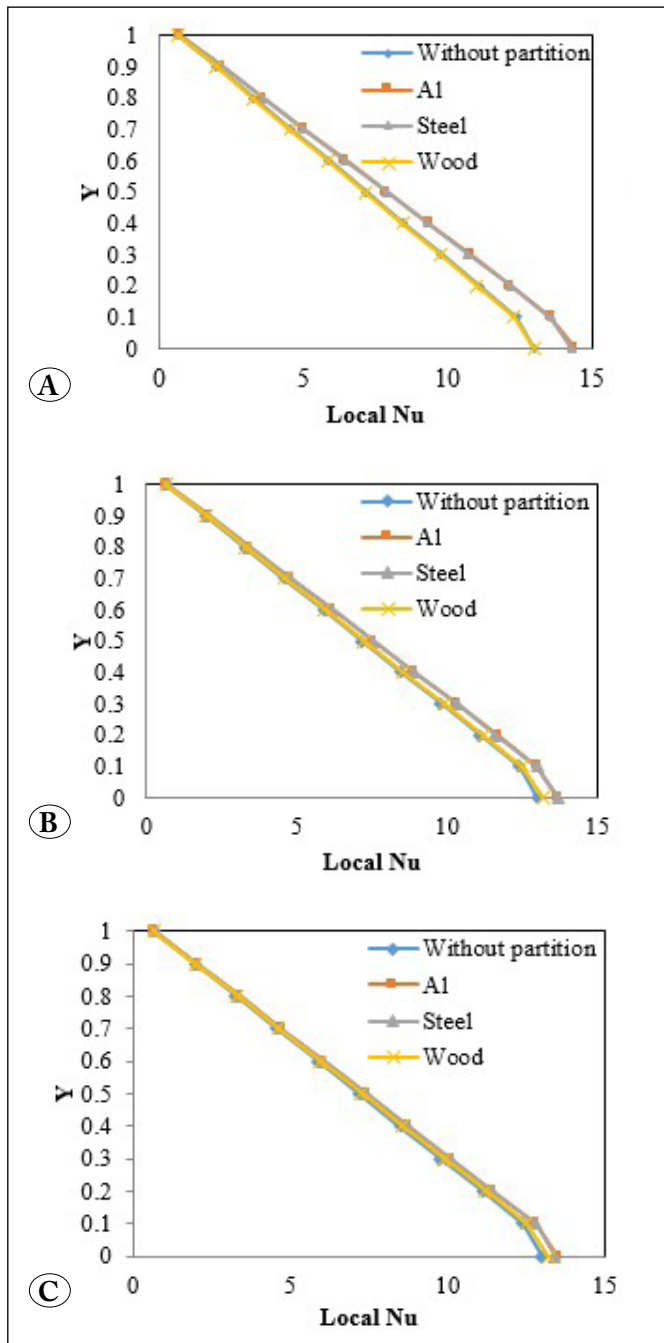


**Figure 6.** Variation of local Nusselt number for  $Ra=6 \cdot 10^5$  A)  $R=1$ , B)  $R=1.1$ , C)  $R=1.12$ .

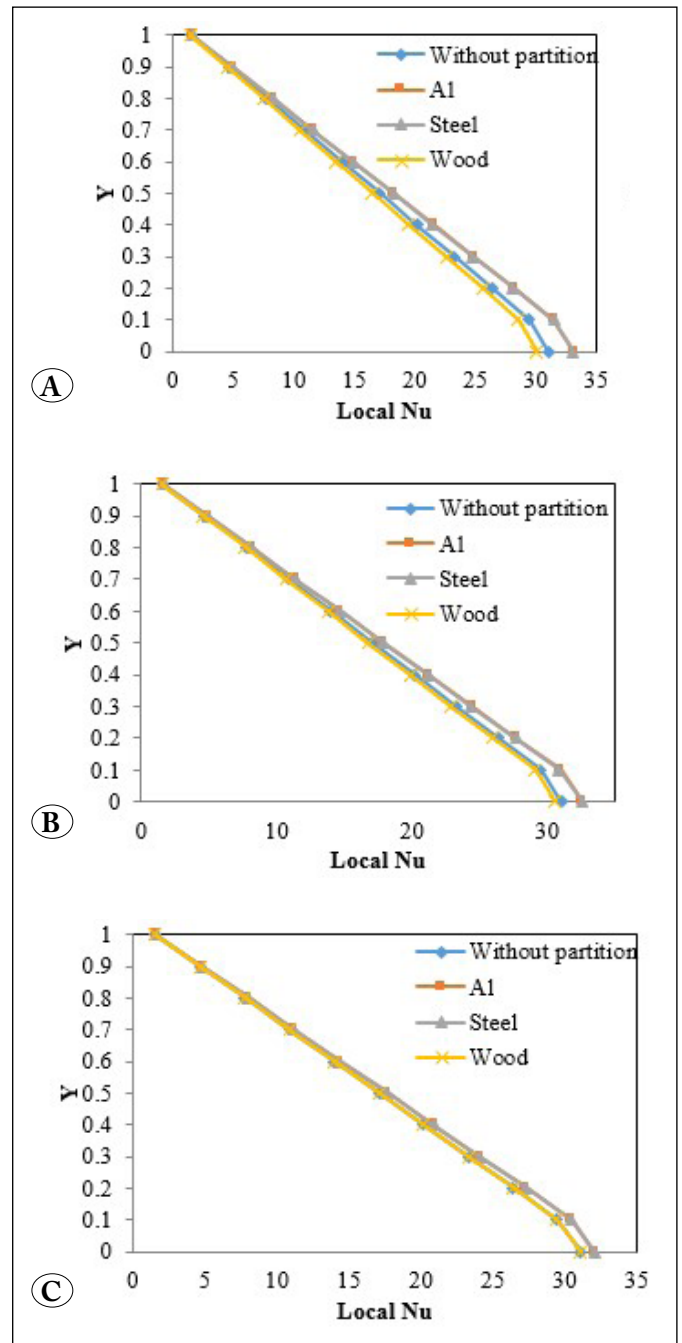


**Figure 7.** Variation of local Nusselt number for  $Ra=4 \cdot 10^6$ , A)  $R=1$ , B)  $R=1.1$ , C)  $R=1.12$ .

## Greek letters

- $\alpha$  thermal diffusivity,  $m^2/s$   
 $\beta$  coefficient of thermal expansion of fluid,  $1/K$   
 $\nu$  kinematic viscosity,  $m^2/s$   
 $\theta$  dimensionless temperature  
 $\rho$  density,  $kg/m^3$

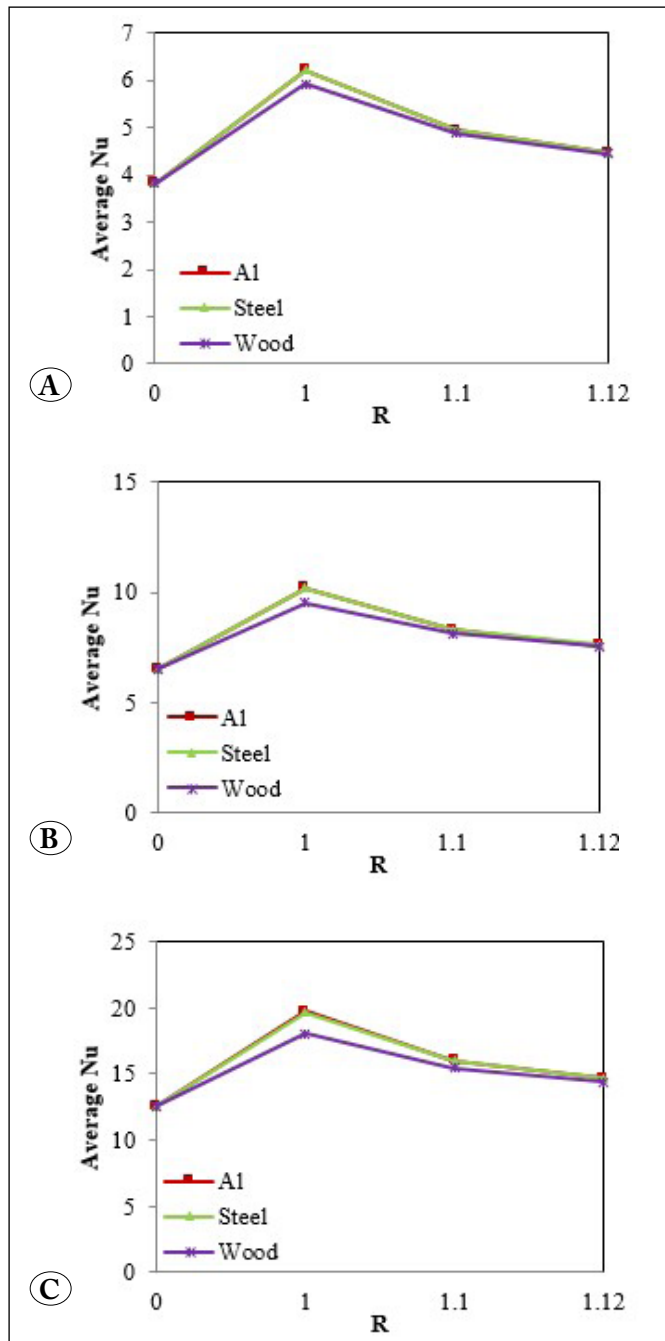


**Figure 8.** Variation of average Nusselt number with different radius and material of partition at different Rayleigh numbers, **A)**  $Ra=7 \cdot 10^4$ , **B)**  $Ra=6 \cdot 10^5$ , **C)**  $Ra=4 \cdot 10^6$

## 5. References

- Al-Amiri A., Khanafer K., Pop I. 2009.** Buoyancy-induced flow and heat transfer in a partially divided square enclosure. *Int. J. Heat Mass Transfer*, 52:3818-3828.
- Barakos G., Mitsoulis E., Assimacopoulos D. 1994.** Natural convection flow in a square cavity revisited: laminar and turbulent models with wall functions. *Int. J. Num. Meth. Fluids*, 18:695-719.
- Costa V.A.F., Oliveira M.S.A., Sousa A.C.M. 2003.** Control of laminar natural convection in differentially heated square enclosures using solid inserts at the corners. *Int. J. Heat Mass Transfer*, 46:3529-3537.
- Costa V.A.F. 2012.** Natural convection in partially divided square enclosures: Effects of thermal boundary conditions and thermal conductivity of the partitions. *Int. J. Heat Mass Transfer*, 55:7812-7822.
- Chamkha A.J., Ismail M.A. 2013.** Conjugate heat transfer in a porous cavity filled with nanofluids and heated by a triangular thick wall. *Int. J. Thermal Sci.* 67:135-151
- Chamkha A.J., Ismail M.A. 2013.** Conjugate heat transfer in a porous cavity heated by triangular thick wall, *Numerical Heat Transfer, Part A*, 63:144-158.
- Fluent 2009.** 12.0 User Guide.
- Hayase J., Humphrey A. C., Greif A. R. 1992.** A Consistently formulated QUICK scheme for fast and stable convergence using finite-volume iterative calculation procedures, *J. Comp. Physics*, 98:108-118.
- Kuznetsov G.V., Sheremet M.A. 2010.** Numerical simulation of turbulent natural convection in a rectangular enclosure having finite thickness walls. *Int. J. Heat Mass Transfer*, 53:163-177.
- Lin N.N., Bejan A. 1983.** Natural convection in a partially divided enclosure. *Int. J. Heat Mass Transfer*, 26: 1867-1878.
- Nishimura T., Nagasawa F., Kawamura Y. 1989.** Natural convection in horizontal enclosures with multiple partitions. *Int. J. Heat Mass Transfer*, 32:1641-1647.
- Oztop H.F., Fu Z., Yu B., Wei J. 2011.** Conjugate natural convection in air filled tube inserted a square cavity. *Int. Comm. Heat Mass Transfer*, 18:580-586.
- Patankar S.V. 1980.** *Numerical Heat Transfer and Fluid Flow*, Hemisphere, New York.
- Tasnim S. H., Collins M. R.. 2005.** Suppressing natural convection in a differentially heated square cavity with an arc shaped baffle. *Int. Comm. Heat Mass Transfer*, 32:94-106.
- Wan D.C., Patnaik B.S.V., Wei G.W. 2001.** A new benchmark quality solution for the buoyancy-driven cavity by discrete singular convolution. *Num. Heat Transfer, Part B*, 40:199-228.